HORIZON EXPANSION OF THERMAL-HYDRAULIC ACTIVITIES INTO HTGR SAFETY ANALYSIS INCLUDING GAS-TURBINE CYCLE AND HYDROGEN PLANT

HEE CHEON NO*, HO JOON YOON, SEUNG JUN KIM, BYENG JIN LEE, JI HWAN KIM, HYEUN MIN KIM and HONG SIK LIM[1]
Department of Nuclear and Quantum Engineering,
Korea Advanced Institute of Science and Technology, Korea
[1] Korea Atomic Energy Research Institute
*Corresponding author. E-mail : hcno@kaist.ac.kr

Invited March 28, 2008
Received October 30, 2008

We present three nuclear/hydrogen-related R&D activities being performed at KAIST: air-ingressed LOCA analysis code development, gas turbine analysis tool development, and hydrogen-production system analysis model development. The ICE numerical technique widely used for the safety analysis of water-reactors is successfully implemented into GAMMA, with which we solve the basic equations for continuity, momentum conservation, energy conservation of the gas mixture, and mass conservation of 6 species (He, N2, O2, CO, CO2, and H2O). GAMMA has been extensively validated using data from 14 test facilities. We developed a tool to predict the characteristics of HTGR helium turbines based on the throughflow calculation with a Newton-Raphson method that overcomes the weakness of the conventional method based on the successive iteration scheme. It is found that the current method reaches stable and quick convergence even under the off-normal condition with the same degree of accuracy. The dynamic equations for the distillation column of HI process are described with 4 material components involved in the HI process: H2O, HI, I2, H2. For the HI process we improved the Neumann model based on the NRTL (Non-Random Two-Liquid) model. The improved Neumann model predicted a total pressure with 8.6% maximum relative deviation from the data and 2.5% mean relative deviation, and liquid-liquid-separation with 9.52% maximum relative deviation from the data.

KEYWORDS : HTGR, Thermal-hydraulic, Safety Analysis, Gas-turbine, Hydrogen Plant

1. INTRODUCTION

A hydrogen economy will need significant new sources of hydrogen. One of the promising approaches to efficiently produce large quantities of hydrogen from nuclear energy is the Sulfur-Iodine (S-I) thermochemical water-splitting cycle, driven by high temperature heat from a helium Gas-Cooled Reactor. The typical thermal-hydraulic activities are expanded starting from typical water reactor-related R&D activities into nuclear/hydrogen-related R&D activities. Here, we present three nuclear/hydrogen-related R&D activities being performed at KAIST: air-ingressed LOCA analysis code development, hydrogen-production system analysis model development, and gas turbine analysis tool development.

1.1 Governing Equations and Numerical Method

The governing equations consist of the basic equations for continuity, momentum conservation, energy conservation of the gas mixture, and mass conservation of 6 species (He, N2, O2, CO, CO2, and H2O). The governing equations are discretized in a semi-implicit manner in a staggered mesh layout and dependent variables are then linearized by the Newton method. For fast computation, the Implicit Continuous Eulerian (ICE) technique is adopted in order to reduce a 10N*10N matrix to a N*N pressure difference matrix. The calculation procedure of the program follows eight major steps, as shown in Fig 1. Detailed descriptions of the governing equations and the numerical technique are given in refs. [1-3].

1.2 Physical Models of GAMMA

For the system analysis code developed to predict the important phenomena expected to occur during thermo-fluid transients, including an air ingress accident, in HTGRs, the following requirements should be considered:

- **Fluid transport and material properties.** The accurate prediction of gas or gas-mixture properties is a basic requirement for analyzing gas flow, heat transfer, and mass transfer. Also, accurate representation

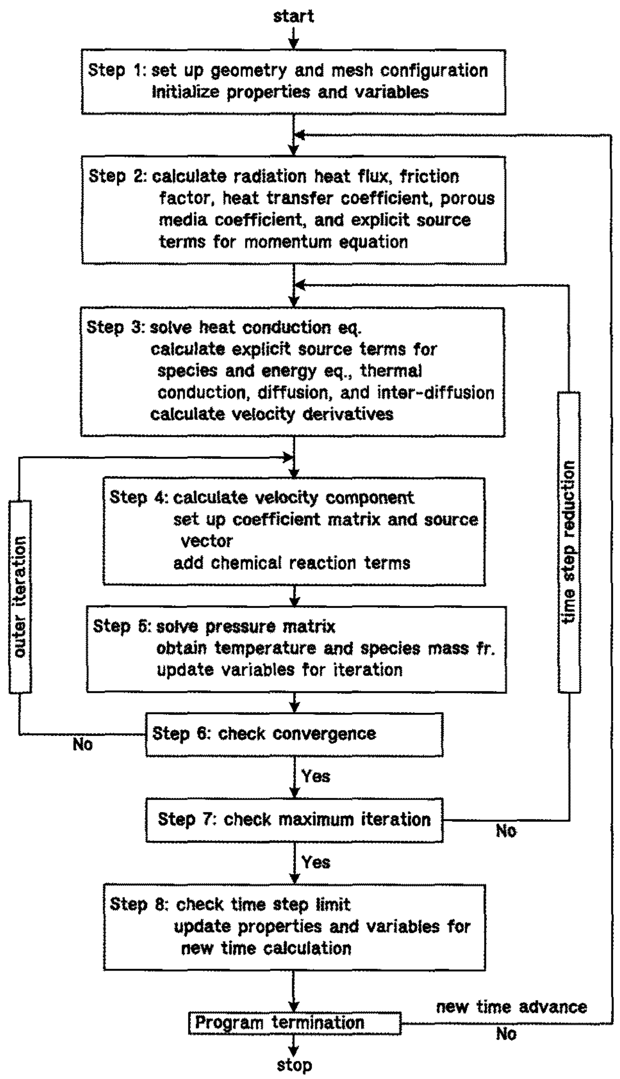

Fig. 1. Calculation Procedure of the Analysis Program

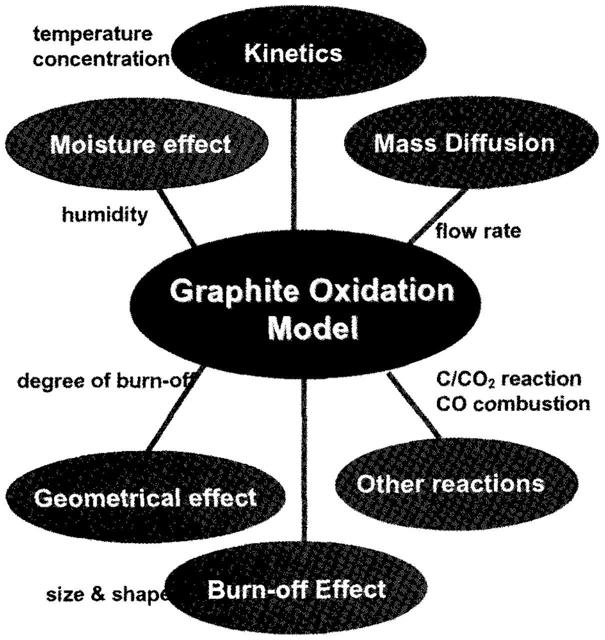

Fig. 2. Development of Models for Rate of Graphite Oxidation

of conductivity and specific heat of the fuel and reflectors is needed to ensure local temperature distribution.

- **Multi-dimensional heat conduction.** Accurate prediction of the local temperature distribution in a complex geometry is necessary to ensure local hot spot and reactivity feedback.
- **Multi-dimensional fluid flow.** A non-uniform and asymmetric flow may result in local hot spot in the core. A natural circulation inside the core is one of the core cooling mechanisms during postulated accidents. A natural circulation inside the reactor cavity partly contributes to RCCS heat removal.
- **Chemical reactions.** The accurate prediction of bulk CO reaction is necessary to ensure species concentration and the onset of bulk natural circulation. The graphite surface oxidation is evaluated to determine temperature rise by air-ingress.
- **Multicomponent molecular diffusion.** The molecular diffusion in a multicomponent mixture system is evaluated to determine the buoyancy force and eventually the onset time of natural convection.
- **Fluid heat transfer and pressure drop.** The accurate representation of pressure drop and heat transfer is necessary to ensure an adequate flow rate and flow distribution and heat removal rate, respectively.
- **Heat generation and dissipation.** The core power and the heat produced from the graphite oxidation are the heat source that determines the consequent temperature transients.
- **Radiation heat transfer.** The accurate prediction of radiation heat transfer in a complex geometry is necessary to ensure adequate heat removal from the core to the RCCS.

In GAMMA extensive graphite oxidation models are developed to include several phenomena and effects on reaction rates, as shown in Fig 2: a kinetics model, mass diffusion model, geometrical, moisture, and moisture effects.

In order to investigate which numerical scheme between the ICE and SIMPLE numerical schemes is a better option for the safety analysis of HTGRs, the tool developed here on the basis of the ICE numerical scheme is compared with FLUENT6 [4], a CFD code based on the SIMPLE numerical scheme. We used an inverse U-tube test apparatus [5], through which isothermal and non-isothermal tests are conducted. The predictions agree well within a 10% deviation with the experimental data. When a 900 MHz

Table 1. Assessment Matrix for GAMMA Verification and Validation

No.	Test Facility	Phenomena
1	Pipe Network, North West Univ., SA	Flow balancing in a complex pipe network
2	Blowdown, North West Univ., SA	Pressure transient and critical flow
3	Duncan & Toor's experiment	Multicomponent molecular diffusion
4	Inverse U-tube single/multiple channel test	Binary molecular diffusion and natural convection
5	Ogawa's circular tube test	Chemical reactions in a IG-110
6	Takahashi's annular tube test	Chemical reactions in a IG-110
7	VELUNA pebble bed test	Chemical reactions in a pebble bed
8	Inverse U-tube air ingress experiment	Molecular diffusion, natural convection, and chemical reactions
9	HTTR-simulated air ingress experiment	Molecular diffusion, natural convection, and chemical reactions Multi-D effect on air ingress process
10	Vertical slot experiment	Local circulation effect on molecular diffusion
11	NACOK natural convection test	Natural convection in a pebble bed
12	SANA-1 afterheat removal test	Pebble temperature distributions: steady power tests and power ramp up/down tests
13	HTTR RCCS mockup test	Air convection and radiation in a reactor cavity
14	SNU RCCS test	Air convection and radiation in a reactor cavity

Pentium III PC is used for the simulation, the FLUENT calculation takes almost 40 times longer than the present model even though the number of mesh elements used in the FLUENT calculation is about twice that in the present model.

Table 1 lists all the test cases collected for the verification and validation of the GAMMA code to ensure the GAMMA capability to predict the basic physical phenomena expected during the transients in a HTGR. GAMMA has been validated against an extensive database.

2. GAS TURBINE ANALYSIS USING THROUGHFLOW METHOD

The real flow in an axial flow multi-stage compressor is inherently three-dimensional and exceedingly complex. Therefore, it is necessary to simplify the flow as having an intermediate level of sophistication. To date, axisymmetric throughflow analyses are generally used in the design and analysis of flows in compressors. For the throughflow calculation a two-dimensional inviscid analysis is performed on a set of streamlines on a hub to tip plane through an arbitrary number of segments of the turbo machine. Recently, the three-dimensional calculation of a flow has become possible using computational fluid dynamics (CFD) codes. However, performing a full calculation for a three-dimensional viscous flow is very laborious and takes considerably longer time for multi-stage calculations and frequent use. Also, for a transient analysis, it is necessary to couple CFD codes with the transient system code. On the other hand, the throughflow calculation provides sufficiently reliable information to allow us to proceed with simple and effective changes to the design. It is relatively easy to couple the code based on the throughflow method with the system code and it takes relatively small computation time to run the coupled code for the transient system analysis. For these reasons, the throughflow calculations are an essential part of the conceptual design and the off-design analysis.

Several throughflow methods have been developed. They are based on the approaches of successive approximations with relaxation techniques, which can result in a convergence problem during the transient analysis. We developed a method to predict the characteristics of HTGR helium turbines based on a throughflow calculation with a new numerical application that overcomes the weakness of the conventional method.

There is a common aspect between the mean-line approach and throughflow approach: the flow direction of relative velocity is the same as the tangential slope on the inner surface of a stator or rotor. Meanwhile, there are differences between the velocity diagram approach and throughflow approach:

1. The throughflow approach considers the contribution of the radial component of velocity while the velocity diagram approach neglects this.
2. Throughflow approach considers a nonuniform axial

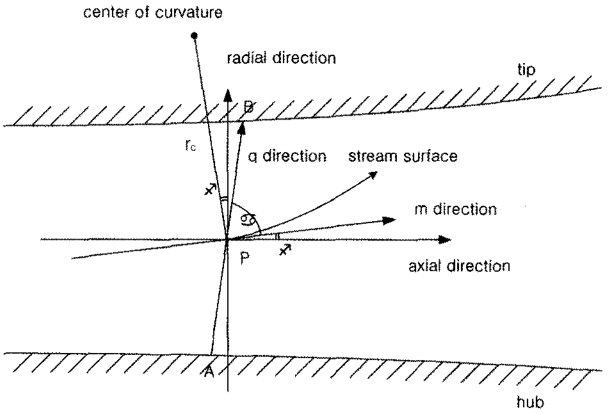

Fig. 3. Schematics of Coordinates for Throughflow Analysis

velocity profile in each axial position while the velocity diagram approach considers a uniform axial velocity profile with one representative velocity. The axial velocity slightly shifts to the tip in the stator and slightly shifts to the hub in the rotor in the turbine. The nonuniform distribution of the axial velocity causes a reduction in work capacity.

The main characteristics of the throughflow analysis are as follows:

1. The use of natural coordinates (q,m) instead of cylindrical coordinates (r,q,z), as shown in Fig. 3, with the following assumptions of inviscid and axisymmetric flows. Here, the coordinates m and q represent the streamline tangential direction at the edges of blades and the blade leading-edge and trailing-edge directions, respectively, as shown in Fig. The streamline is produced so that the mass flow rate between each one will be the same. The coordinate transformation renders the two momentum equations in the r and z directions based on cylindrical coordinates into one transformed momentum equation in the q direction.
2. Solution of the radial equilibrium equation combining the one transformed momentum equation and energy equations through the elimination of pressure. Now, we only have two equations to be solved: the radial equilibrium equation and continuity equation

Here, we summarize the derivation for the throughflow analysis based on J.D. Denton (1978)[6] as follows: Starting from the following Navier-Stokes momentum and energy equations

$$\frac{\partial \mathbf{W}}{\partial t}+\frac{1}{2}\nabla W^2-\mathbf{W}\times(\nabla\times\mathbf{W})-\mathbf{r}\omega^2+2\omega\times\mathbf{W}=-\frac{1}{\rho}\nabla p+\mathbf{F}_b \tag{1}$$

where W: relative velocity, ω = rotational speed, F_b: blade force, we obtain 2 momentum equations in the r- and z-directions with the assumptions of inviscid and axisymmetric flows for the stator and rotor, respectively.

r-direction :

$$W_r\frac{\partial W_r}{\partial r}+W_z\frac{\partial W_r}{\partial z}-\frac{1}{r}(W_\theta+\omega r)^2=-\frac{1}{\rho}\frac{\partial p}{\partial r}+F_b\big|_r \tag{2}$$

Z-direction:

$$W_r\frac{\partial W_z}{\partial r}+W_z\frac{\partial W_z}{\partial z}=-\frac{1}{\rho}\frac{\partial p}{\partial z}+F_b\big|_z \tag{3}$$

The two momentum equations are combined to form one momentum equation through a coordinate transformation from (r,z) into a streamline curvature coordinate (q)

$$-\frac{1}{\rho}\frac{\partial p}{\partial q}+F_b\big|_q=-\frac{(W_\theta+\omega r)^2}{r}\sin(\alpha+\phi)+W_m\frac{\partial W_m}{\partial n}\cos\alpha+\frac{W_m^2}{r_C}\sin\alpha \tag{4}$$

The one energy equation is converted into the following equation through a coordinate transformation from (r,z) into a streamline tangential coordinate (q):

$$\frac{1}{\rho}\nabla p=\nabla h-\frac{1}{2}\nabla\left(V_m^2+V_\theta^2\right)-T\nabla s \tag{5}$$

The coordinate-transformed momentum and energy equations are combined by eliminating pressure. We then have the radial equilibrium equations for stationary and rotating frames. The radial equilibrium equation for stationary frame is as follows:

$$\frac{1}{2}\frac{d}{dq}V_m^{\ 2}=\frac{dh_0}{dq}-T\frac{ds}{dq}+a_q \tag{6}$$

where

$$a_q=-\frac{1}{2r^2}\frac{d\left(r^2V_\theta^2\right)}{dq}+\frac{V_m^2}{r_c}\sin\alpha+V_m\frac{dV_m}{dm}\cos\alpha \tag{7}$$

This radial equilibrium equation is the basis of all throughflow calculation methods. Equation (6) must be solved in conjunction with the continuity equation as follows:

$$\dot{m}=\int_{hub}^{tip}2\pi rb\rho V_m\sin\alpha\, dq \tag{8}$$

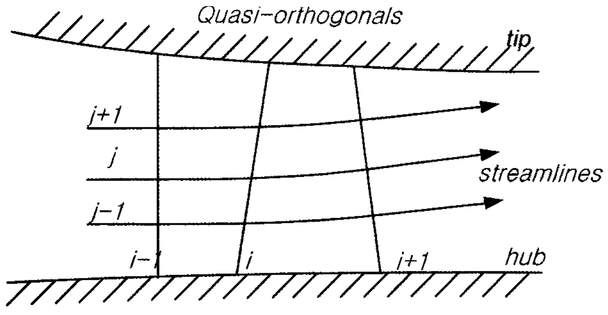

Fig. 4. Grid Generation

where ***b*** is a measure of blockage and would be unity in an ideal case.

In order to estimate a tangential component of the absolute velocity, we need to start from the following angular momentum conservation equation between torque on the blades and the net torque from entering and leaving flows:

$$\dot{W} = \tau\omega = \dot{m}\omega(V_{\theta 1}r_1 - V_{\theta 2}r_2) \tag{9}$$

We then have the following Euler-turbo equation:

$$\dot{W}/\dot{m} = (h_{01} - h_{02}) = \omega(V_{\theta 1}r_1 - V_{\theta 2}r_2) \tag{10}$$

In most gas turbine designs, the following free vortex design concept is used for the estimation of a tangential component of the absolute velocity:

$$rV_\theta = \frac{power\ per\ stage}{\dot{m}_{inlet} \times \omega} \tag{11}$$

A numerical grid for the throughflow calculations is generated by the intersections of each streamline and each quasi-orthogonal. Fig. 4 shows a schematic of the grid generation. The quasi-orthogonal lines are denoted by i-nodes, and the streamlines are denoted by j-nodes. The blade force and the blockage factor can be neglected in the simplified case.

The following radial equilibrium equation multiplied by dq gives the difference of V_m^2 between two adjacent streamtubes.

$$\frac{1}{2}\delta\left(V_m^{\,2}\right) = \delta h_0 - T \times \delta s - \frac{\delta\left(rV_\theta\right)^2}{2r^2} + V_m^{\,2}\delta r \times SCT \tag{12}$$

where

$$\delta(V_m)_j^{\,2} = (V_m)_{j+1}^{\,2} - (V_m)_j^{\,2}$$

$$SCT = \frac{1}{\sin\left(\alpha+\phi\right)}\left(\frac{1}{r_c}\sin\alpha + \frac{1}{V_m}\frac{dV_m}{dm}\cos\alpha\right)$$

The term SCT is calculated separately and updated later for the whole machine.

The mass flow rate is expressed as the sum of flow rates between two adjacent streamlines:

$$\dot{m} = \sum_{j=1}^{J}\delta\dot{m} = \sum_{j=1}^{J}\frac{2\pi\delta r_j}{\sin(\alpha+\phi)_j} \times \rho r V_{mj}\sin\alpha_j \tag{13}$$

where r_j is the streamline position.

The velocity in the θ direction is estimated by solving the Euler-turbo equation using the free vortex condition (constant stage power). We developed the Newton-Raphson method to solve the radial equilibrium term of equation (12) and the continuity equation simultaneously. The conventional method applies a successive iteration scheme to this end. The linearization of these two equations leads to the matrix equation AX=-B. V_{mj} and r_j can then be evaluated simultaneously. It is found that the current method reaches a stable and quick convergence even under the off-normal condition with the same degree of accuracy [7].

3. HYDROGEN-PRODUCTION SYSTEM ANALYSIS MODEL DEVELOPMENT: THERMO-CHEMICAL PROCESS IN THE REACTIVITY DISTILLATION COLUMN

Because of high and unstable oil prices, as well environmental reasons, nuclear-hydrogen production techniques have been developed in several countries. In the 1980s General Atomics Co [8] proposed a promising method known as the IS (Iodine-Sulfur) thermochemical water-splitting cycle. It utilizes the following multi-step water splitting process:

Section I (Bunsen reaction) - Exothermic

$$(9I_2)_l + (SO_2)_g + (16H_2O)_l \Rightarrow (2HI + 10H_2O + 8I_2)_l + (H_2SO_4 + 4H_2O)_l \quad (393K), \tag{14}$$

Section II (Decomposition of HI acid in lower layer) - Endothermic

$$L_2 = (2HI + 10H_2O + 8I_2)_l \Rightarrow (2HI)\,g + (10H_2O + 8I_2)_l \quad (500K), \tag{15}$$

$$(2HI)\,g \Rightarrow H_2 + (I_2)_l \quad (600K), \tag{16}$$

Section III (Decomposition of sulfuric acid in upper layer) - Endothermic

$$L_1 = (H_2 + SO_4 + 4H_2O)_l \Rightarrow (H_2SO_4)_l + (4H_2O)_l \quad (570K), \tag{17}$$

$$(H_2SO_4)_l \Rightarrow (H_2SO_4)\,g \quad (630K), \tag{18}$$

$$(H_2SO_4)\,g \Rightarrow (SO_3)g + (H_2O)\,g \quad (670K), \tag{19}$$

$$(SO_3)\,g \Rightarrow (SO_2)\,g + 1/2\,O_2 \quad (1140K), \tag{20}$$

The IS process uses several distillation columns in which thermo-chemical phenomena governs its performance and transient behavior. The typical column contains several parts: trays/plates and/or packings for enhancing separation, a reboiler for vaporization, a condenser for condensing the vapor leaving the top of the column, and a reflux drum where liquid can be recycled back to the column.

There are many types of tray designs, but the most common is a bubble cap tray, which has a riser fitted over each hole, and a cap that covers the riser. Each tray has two downcomers through which liquid falls by gravity from one tray to the one below it. A weir on the tray functions as a holdup where some liquid will be held on the tray at a suitable height. When the hotter vapor passes through the liquid on the tray above, mass and energy transfer takes place between it and the liquid. Through its condensation, the condensate is richer in less volatile components than is the vapor. Also, through energy transfer, the liquid on the tray boils, generating more vapor that moves up to the next tray in the column. As a result, the vapor is richer in more volatile components. This is called a separation process between low boiling point and higher boiling point component. Optimal trays are designed to maximize vapor-liquid contact by considering the liquid and vapor distributions on the tray.

In the reactivity distillation column, there are no active components. Therefore, counter-current flow takes place: liquid falls down by gravity and vapor flows upwards

Four flow conditions exist: foaming, entrainment, weeping/dumping, and flooding. Foaming represents the expansion of liquid due to passage of vapor or gas. Excessive foaming often leads to liquid buildup on trays, while it provides high interfacial liquid-vapor contact. In weeping, the pressure exerted by the low vapor flow is insufficient to hold the liquid on the tray and, as a result, the liquid starts to leak through perforations. Excessive weeping will lead to dumping. Flooding resulting from excessive vapor flow causes the liquid to be entrained in the vapor located higher in the column. The increased pressure from excessive vapor backs up the liquid in the downcomer, causing an increase in liquid holdup on the plate above.

3.1 Dynamic Thermo-chemical Models

There are two main dynamic thermo-chemical models:

1. Equilibrium (EQ) stage model
2. Nnequilibrium (NEQ) stage model

In the Equilibrium (EQ) stage model, vapor from the stage below and liquid from the stage above are brought into contact on the stage together with any fresh or recycle feeds. The vapor and liquid streams leaving the stage are assumed to be in thermal-chemical equilibrium with each other. The dynamic thermo-chemical models conventionally used in chemical engineering do not use momentum equations for the prediction of vapor and liquid velocities inside the column, but we consider the pressure drop through the stages or assume a constant column pressure.

$$P_j - P_{j-1} - (\Delta P_{j-1}) = 0 \tag{21}$$

where P_j and P_{j-1} are the stage pressures in j and j-1 stages, and ΔP_{j-1} is the pressure drop per tray from stage (j-1) to stage j.

Simple momentum equations are used for the estimation of the time variation of flow between two tanks, icolumn and jcolumn:

$$P_{icolumn} - P_{jcolumn} = K_{ij} 1/2(\rho V^2)_{ij} \tag{22}$$

This raises the question of how it is possible to obtain the liquid and vapor flows without solving the momentum equations, which should be solved in the safety analysis of water reactors. The vapor flow is governed by the following balance:

Vapor flow = feed vapor flow + refluxing vapor flow
+ vapor production rate from liquid
– Vapor destruction rate to vapor

Vapor production rates are determined by evaporation through phase transformation, heat in, and depressurization. Vapor destruction rates are determined by condensation through phase transformation from the vapor to liquid, heat out, and pressurization. If the transient effects of the vapor phase on mass and energy are small, the gas flow rate out of a node even in a transient simulation can be safely assumed to be the same as the vapor production rate. As a result, we do not need to solve the momentum equation. It is the same in a PWR, where the steam flow rate $\dot{m}_{SG}$ out of the steam generator is governed by the vapor generation rate by heat transfer $\dot{Q}_{SG}$ from the primary side in the steam generator.

$$\dot{m}_{SG} = \dot{Q}_{SG}/(h_s - h_F) \tag{23}$$

Liquid flow is then estimated in the same manner as vapor flow:

liquid flow = feed liquid flow + refluxing liquid flow
+ liquid production rate from vapor
destruction – liquid destruction rate to vapor

The essence of the non-equilibrium stage model is the method to deal with mass transfer at the vapor-liquid interface. Mass transfer at the vapor-liquid interface is described via the well-known two-film model. The Maxwell-Stefan equations are used to model multi-component diffusion within the films. When we have to deal with the chemical reaction in the film regions, the model becomes more complicated.

The dynamic equations for the distillation column of the HI process are described in a simplified way. For a simple description, the column consists of one boiler and one condenser, denoted here as subscripts 0 and 1.There are 4 material components involved in the HI process: H2O, HI, I2, and H2, denoted here as subscripts a, b, c, and d, respectively. As the transient effects of the vapor phase region on mass and energy are much smaller than those of the liquid phase region, we only consider the temporal variation of the liquid mass in the liquid phase region. As a result, the gas flow rate out of a node even in the transient simulation can be safely assumed to be the same as the vapor production rate. The following overall material balance, component material balance, energy balance equations, and hydraulic equation are used in the column.

1. condenser

$$\begin{aligned}
&dM_{L1}/dt = -V_1 + L_0 - B + F \\
&dM_{L1}x_{a,1}/dt = -V_1 y_{a,1} + L_0 x_{a,0} - Bx_{a,1} + Fx_{a,F} + R_{a,1} \\
&dM_{L1}x_{b,1}/dt = -V_1 K_{b,1} x_{b,1} + L_0 x_{b,0} - Bx_{b,1} + Fx_{b,F} + R_{b,1} \\
&dM_{L1}x_{c,1}/dt = -V_1 K_{c,1} x_{c,1} + L_0 x_{c,0} - Bx_{c,1} + Fx_{c,F} + R_{c,1} \\
&dM_{L1}h_{L,1}/dt = -V_1 h_{V,1} + L_0 h_{L,0} - Bh_{L,B} + Fh_{L,F} + Q_1 + R_{b,1}\Delta H_b
\end{aligned} \tag{24}$$

2. boiler

$$\begin{aligned}
&dM_{L1}/dt = -V_1 + L_0 - B + F \\
&dM_{L1}x_{a,1}/dt = -V_1 y_{a,1} + L_0 x_{a,0} - Bx_{a,1} + Fx_{a,F} + R_{a,1} \\
&dM_{L1}x_{b,1}/dt = -V_1 K_{b,1} x_{b,1} + L_0 x_{b,0} - Bx_{b,1} + Fx_{b,F} + R_{b,1} \\
&dM_{L1}x_{c,1}/dt = -V_1 K_{c,1} x_{c,1} + L_0 x_{c,0} - Bx_{c,1} + Fx_{c,F} + R_{c,1} \\
&dM_{L1}h_{L,1}/dt = -V_1 h_{V,1} + L_0 h_{L,0} - Bh_{L,B} + Fh_{L,F} + Q_1 + R_{b,1}\Delta H_b
\end{aligned} \tag{25}$$

where
L,V,D,B,R: liquid and vapor mole flow rates, distillation rate out of the column, vapor generation rate in the boiler, reaction rate by chemical reaction
Q : energy-in rate
h : enthalpy
M_L: liquid holdup mass

We need the following additional constraints to the above balance equations, called the summation relation:

$$\begin{aligned}
&x_{a,0} + x_{b,0} + x_{c,0} = 1; x_{a,1} + x_{b,1} + x_{c,1} = 1; \\
&y_{a,0} + y_{b,0} + y_{c,0} + y_{d,0} = 1; y_{a,1} + y_{b,1} + y_{c,1} + y_{d,1} = 1
\end{aligned} \tag{26}$$

The distillation rate becomes the hydrogen production rate at a steady state:

$$D = R_{d,1} + R_{d,0} \tag{27}$$

Note that the vapor flow of each component consists two parts: its production rate by liquid evaporation and its production/destruction rate by chemical reaction. To solve these equations, we need the following equilibrium relation between the liquid fraction and gas fraction of each component:

$$y_i = K_i x_i \tag{28}$$

The partial pressure of each gas component is determined by

$$P_{Vi} = y_i P = \gamma x_i P_{sat}(T_L) \tag{29}$$

The models on K and γ play an essential role in the thermochemical process. In the following we describe the models on K and γ for the HI process. We studied the HI process using the Neumann model [9], which is based on the NRTL model. According to the solvation model, m molecules of H2O with one molecule of HI form two complexes:

$$m\,H_2O + HI \longleftrightarrow m\,H_2O + H^+ + I^- \longleftrightarrow C^+ + C^- \qquad (30)$$

The products of ionization of HI, H+ and I-, will interact with polarized H2O molecules.

Because this reaction is very fast we assume an equilibrium state. We then have

$$K_C = (x\gamma)_C^2 / \left[(x\gamma)_{H_2O}^m (x\gamma)_{HI} \right] \qquad (31)$$

In the Neumann model, K_C is empirically determined in terms of temperature:

$$K_C = \exp(A + B/T) \qquad (32)$$

For the computation of the activity coefficients Neumann uses the NRTL (Non-random Two-Liquid) model. In the NRTL model each reciprocal effect between two particle places is reflected by three coefficients: τ_{ij}, τ_{ji}, $\alpha_{ij} = \alpha_{ji}$. For i=j τ_{ij} and α_{ij} are equal to zero. The expression for the activity coefficients is

$$\ln \gamma_i = \frac{\sum_j^N \tau_{ji} G_{ji} x_j}{\sum_j^N G_{ji} x_j} + \sum_k^N \frac{x_k G_{ik}}{\sum_J^N G_{jk} x_j} \left(\tau_{jk} - \frac{\sum_n^N \tau_{nk} G_{nk} x_n}{\sum_J^N G_{jk} x_j} \right) \qquad (33)$$

where

$$G_{ji} = \exp(-\alpha_{ji}\tau_{ji})$$

We need to determine the parameters τ_{ij} and α_{ij}, which are regressed as shown in Fig.5.

The partial pressure of the components in the solution and the total pressure are determined by

$$\begin{aligned} P_{Vi} &= y_i P = \gamma x_i P_{sat}(T_L) \\ P_{total} &= P_{H2O} + P_{HI} + P_{I2} + P_{H2} \end{aligned} \qquad (34)$$

With the following decomposition chemical equation

$$2\mathrm{HI} \longleftrightarrow \mathrm{H_2} + \mathrm{I_2} \qquad (35)$$

we can estimate the hydrogen partial pressure over the relationship for the reaction equilibrium in the vapor phase:

The KAIST model predicted the total pressure with a maximum 8.6% relative deviation from the data and 2.5% mean relative deviation, while Neumann calculated the total pressure with a maximum 7.9% relative deviation and 2.1% mean relative deviation. (Fig. 6)

The prediction result of the LL-separation condition with the improved Neumann's model was evaluated in terms of relative error to the experimental data of Engels and Knoche (Fig. 7). HI concentration for the onset of LL separation can be predicted when the total pressure reaches the saturation pressure of pure HI. Beyond the HI onset concentration the total pressure becomes constant, because almost pure HI exists in the top region of the liquid phase. The present model predicts the flat pressure trend beyond the HI onset concentration. LL-separation is predicted to occur at 32.5% HI concentration when the operating temperature is 100 °C The improved Neumann model predicts that LL-separation will occur at around 29% ~ 34% HI concentration fraction within a temperature range of 70 °C ~ 149 °C The maximum relative deviation in the LL-separation prediction was less than 9.52%.

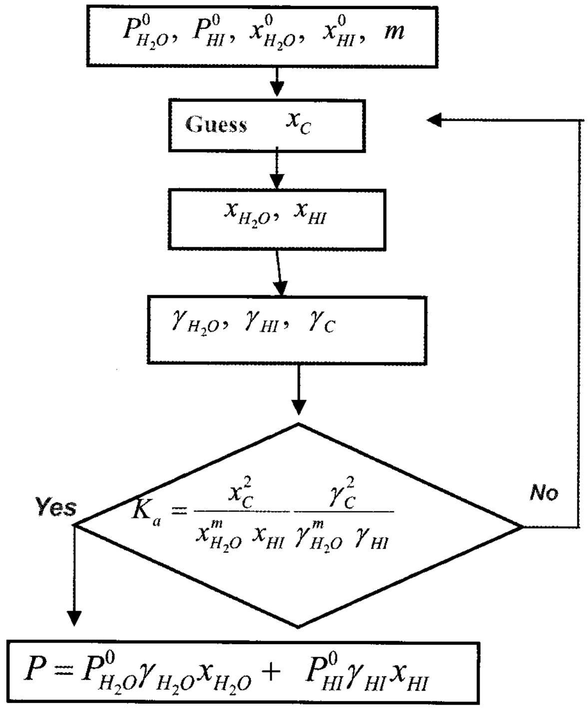

Fig. 5. Regress Flowchart

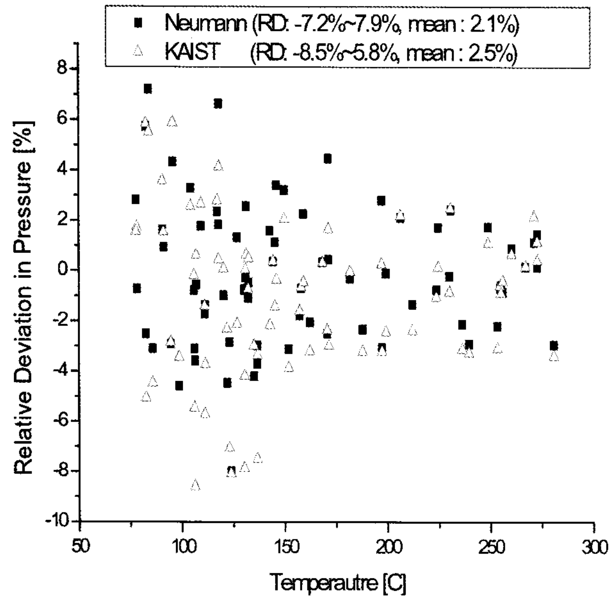

Fig. 6. Comparison of Relative Deviation by KAIST Results with Relative Deviation by Neumann

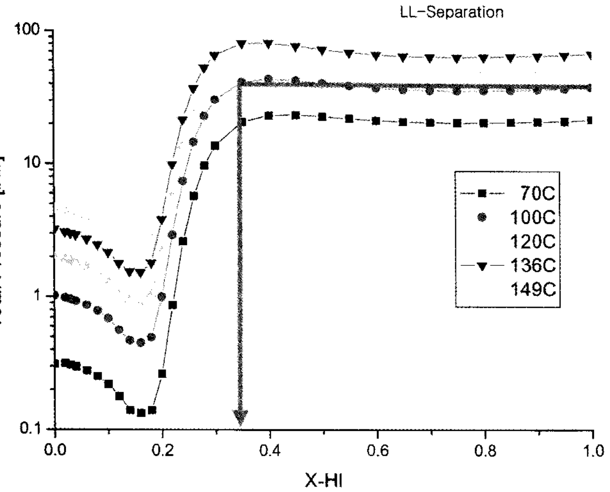

Fig. 7. Total Pressure Calculation with Improved Neumann Model and Liquid-liquid Separation Prediction

3.2 Low Pressure Experiments of HI Process

Sufficient data are needed to develop a precise thermo-physical model in the HI process. The data used in the modified NRTL model is not sufficient around the azeotrope point, as shown in Fig. 9. The present experimental study adds more data and shows thermo physical properties of HI and verifies the NRTL model. For testing the azeotropic restraint, a partial condensing type, a perforated plate type, and packed bed distillation columns are employed. [11] A Liebig-type condenser is used for a partial condensing distillation test. The perforated plate distillation column has 40 mm diameter and 5 stages with 8 holes per plate. The packed bed distillation column has 40 mm diameter and is filled with 5 mm glass beads. Experiments are performed at atmospheric pressure. Test sections basically consist of a reboiler, test columns, a condenser, and a gas capturing bag. The initial sample solution is 0.1583 mol hydriodic acid with no impurities.

Table 2. Change of HI Concentration Fraction

Mol fraction	Partial Condensing Distillation	Perforated Plate Distillation	Packed Bed istillation
Initial solution	0.1575	0.1561	0.1566
Distilled solution	0.1561	0.1561	0.1561
Distilling solution	0.1578	0.1566	0.1577

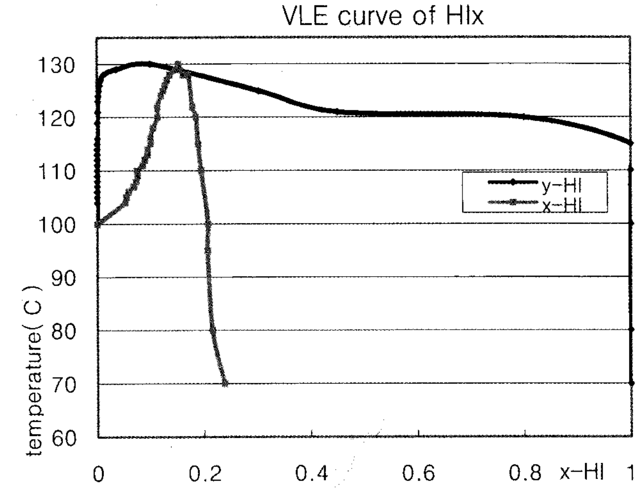

Fig. 8. VLE Curves of HIx

As shown in table 2, the azeotropic restraints are not easily broken up by conventional distillation methods. Attractions between H2O and HI are very strong.

The test section is composed of a 500mL round flask with three necks and a 300 mm Liebig condenser. A PID current controller is used for a heating mantle and a scale for measurement. Under the azeotrope, 20ml sample bottles with a cap are used for measuring the concentration of vapor phase HI acid. 426g of hydroiodic acid with 0.05mole is used as the initial sample solution. Above the azeotrope, 150g of hydroiodic acid with a 0.23 mole fraction is used. To obtain the VLE curve, the mole fractions of vapor and liquid are measured with temperature simultaneously.

The results are shown in Fig. 8. The VLE curve shows that excessive components (H2O or HI) distilled from the complex first and the complex then evaporated. This means

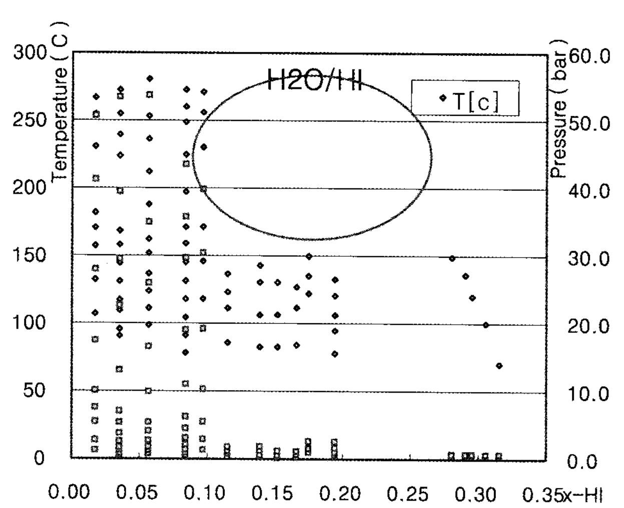

Fig. 9. The Binary Data for Modified NRTL

that HI exists only as a complex in the liquid and vapor phases under azeotropic points. Water exists only as a complex in the liquid and vapor phases above the azeotropic points. Under the azeotropic point, water has a tendency to escape while above the azeotropic point, HI has a tendency to escape. A small deviation of the mole fraction of HI from the azeotrope point leads to evaporation of excessive components.

The modified NRTL model uses four sets of data. [9] One part is the binary solution of H2O/HI. The others are the ternary solution of H2O/HI/I2. Fig. 9 is produced based on the database obtained by Aachen. [12] and JAEA.

As shown in Fig. 9, data around the azeotrope at high temperature and high pressure did not exist, and therefore extrapolation is needed to predict the model. This can lead to increased uncertainties in the model. In order to prevent a corrosion problem, silicon carbide and Hastelloy-C were considered. SiC has better strength than steel. However, the lower ductility of SiC reduces the safety margin. Hastelloy-C shows high corrosion resistance and can be used as an autoclave material and for thermocouple protection. KAIST test data sets will consist of binary and ternary solution properties and verify the current model and suggest experimental correlations.

4. CONCLUSIONS

Here, three nuclear/hydrogen-related R&D activities being performed at KAIST are described: air-ingressed LOCA analysis code development, gas turbine analysis tool development, and hydrogen-production system analysis model development. It is shown that the ICE numerical technique widely used for the safety analysis of water-reactors is successfully implemented into GAMMA. It is found that the current method for the gas-turbine performance analysis based on the throughflow calculation with a Newton-Raphson method reaches a stable and quick convergence even under the off-normal condition with the same degree of accuracy. The improved Neumann model based on the NRTL model predicted the total pressure with a maximum 8.6% relative deviation and 2.5% mean relative deviation, and liquid-liquid-separation with 9.52% maximum relative deviation.

ACKNOWLEDGMENTS

This work was performed under the National Research Laboratory (NRL) Project. Financial support by the Ministry of Science and Technology (MOST) is gratefully acknowledged.

REFERENCES

[1] Hong Sik Lim, Hee Cheon NO, "GAMMA multidimensional multicomponent mixture analysis to predict air ingress phenomena in an HTGR," *Nucl. Sci. Eng.* **152**, 1. (2006)

[2] Hong Sik Lim, Hee Cheon NO, "Transient multicomponent mixture analysis based on an ICE numerical technique for the simulation of an air ingress accident in a HTGR," J. *KNS* **36**, 375 (2004)

[3] Hee Cheon NO, et al., "Multi-component Diffusion Analysis and Assessment of GAMMA code and Improved RELAP5 Code," *Nucl. Eng. & Des.*, **237** (2007)

[4] FLUENT 6.0 User's Guide, *FLUENT Inc.*, 2002.

[5] M. Hishida and T. Takeda, "Study on air ingress during an early stage of a primary-pipe rupture accident of a high-temperature gas-cooled reactor," *Nucl. Eng. & Des.*, **126**, 175 (1991)

[6] J.D. Denton, "Throughflow Calculation for Transonic Axial Flow Turbines", Journal of Engineering for Power, *Transactions of the ASME*, **Vol. 100**, pp. 212-218, 1978.

[7] Hee Cheon NO, Ji Hwan Kim and Hyeun Min Kim, "A Review of Helium Gas Turbine Technology for High-Temperature Gas-Cooled Reactors", *Nuclear Eng. and Tech.*, **Vol. 39**, No 1, 2007

[8] J. H. NORMAN et al, "Thermo-chemical water-splitting cycle, bench-scale investigations, and process engineering - final report for the period February 1977 through December 31, 1981", *General Atomics Report GA-A16713, DOE Report DOE/ET/26225-1*

[9] D. NEUMANN, Phasengleichgewichte von HJ/H2O/J2-Lösungen, Thesis, *Lehrstuhl für Thermodynamik, RWTH Aachen*, 5100 Aachen, Germany, January 1987

[10] M. Roth and K. F. Knoche, "Thermochemical Water-Splitting through Direct HI-Decomposition from H2O/HI/I2 Solutions," *Int. J. Hydrogen Energy* **14**, pp545-549, 1989.

[11] Ho Joon Yoon, "Experiments of HI decomposition in Iodine-Sulfur process", Master Thesis, *Korea Advanced Institute of Science and Technology*, 2006

[12] H. Engels, K.F. Knoche, "Vapor pressures of the systemH2O-HI-I2 system and H2," *Int. J. Hydrogen Energy* **11** (1986) 703-707.

[13] C. Berndahauser, K.F. Knoche, "Experimental investigations of thermal HI decomposition from H2O-HI-I2 solutions," *Int. J. Hydrogen Energy* **19** (3) (1989) 239-244.